ORIGINAL RESEARCH

Francesca R. Napoli et al

Microphthalmia and disrupted retinal development due to a *LacZ* knock-in/knock-out allele at the *Vsx2* locus

Francesca R. Napoli[1], Xiaodong Li[1], Alan A. Hurtado[2], Edward M. Levine[1,3]*

[1] Department of Ophthalmology and Visual Sciences

Vanderbilt University Medical Center, Nashville TN 37232

[2]Program in Chemical and Physical Biology

Vanderbilt University, Nashville TN 37232

[3]Department of Cell and Developmental Biology

Vanderbilt University, Nashville TN 37232

*Corresponding Author: ed.levine@vumc.org

Abstract

Visual System Homeobox 2 (*Vsx2*) is a transcription factor expressed in the developing retina that regulates tissue identity, growth, and fate determination. Several mutations in the *Vsx2* gene exist in mice, including a spontaneous nonsense mutation and two targeted missense mutations originally identified in humans. Here, we expand the genetic repertoire to include a *LacZ* reporter allele ($Vsx2^{LacZ}$) designed to express beta-Galactosidase (b-GAL) and simultaneously disrupt *Vsx2* function (knock-in/knock-out). The retinal expression pattern of b-GAL is concordant with VSX2, and the mutant allele is recessive. $Vsx2^{LacZ}$ homozygous mice have congenital bilateral microphthalmia accompanied by defects in retinal development including ectopic expression of non-retinal genes, reduced proliferation, delayed neurogenesis, aberrant tissue morphology, and an absence of bipolar interneurons - all hallmarks of *Vsx2* loss-of-function. Unexpectedly, the mutant VSX2 protein is stably expressed, and there are subtle differences in eye size and early retinal neurogenesis when compared to the null mutant, *ocular retardation J*. We propose that b-GAL expression from the $Vsx2^{LacZ}$ allele is a reliable reporter of VSX2 expression and that the allele exhibits loss-of-function characteristics. However, the perdurance of the mutant VSX2 protein combined with subtle deviations from the null phenotype leaves open the possibility that $Vsx2^{LacZ}$ allele is not a complete knock-out. The $Vsx2^{LacZ}$ allele adds to the genetic toolkit for understanding *Vsx2* function.

Keywords: LacZ, reporter knock-in, Vsx2, Chx10, retina, proliferation, lineage fidelity, neurogenesis, immunohistology

43 # Introduction

44 Visual System Homeobox (VSX) genes encode paired-like homeodomain
45 transcription factors required for visual system development in both vertebrates and
46 invertebrates. Two paralogous genes, *Vsx1* and *Vsx2* (formerly *Chx10*), are present in
47 vertebrates and have distinct roles in eye growth and retinal formation during
48 development. In humans, clinical features of *Vsx1* disruption include keratoconus and
49 visual deficits whereas *Vsx2* disruption include non-syndromic congenital bilateral
50 microphthalmia and blindness. *Vsx2* mutations also cause non-syndromic
51 microphthalmia in other vertebrates. Understanding how *Vsx2* functions and is
52 regulated has provided important insights into ocular development.

53 *Vsx2* expression is activated in the nascent retinal domain during the
54 morphological transition from the optic vesicle to optic cup, remains expressed in retinal
55 progenitor cells (RPCs) through development, and becomes restricted to bipolar cells
56 and Müller glia in the adult retina.[1,2] Consistent with onset of expression, reductions in
57 eye size and defects in retinal development commence soon after optic cup formation in
58 murine *Vsx2* mutants[1,3] and at an equivalent stage in *Vsx2* mutant human organoids.[4] In
59 mice, retinal defects include ectopic expression of non-retinal genes and differentiation
60 programs more akin to neighboring tissues (lineage infidelity), slowed proliferation,
61 delayed onset of neurogenesis, disrupted laminar morphogenesis, and a lack of bipolar
62 cells.[1,3,5–12]

63 Multiple *Vsx2* alleles encoding structural or regulatory variants exist in mice
64 (informatics.jax.org; Quick Search term: Vsx2; Category: Alleles), but most phenotypic
65 characterizations of *Vsx2* disruption in the eye have been done with three protein

66 coding variants. The most extensively studied is the *ocular retardation J* allele (*orJ;*
67 MGI:1856112), a spontaneous mutation that replaces tyrosine at position 176 with a
68 premature stop codon (Fig. 1A).[1,5] Although *Vsx2* mRNA remains expressed in the *orJ*
69 mutant retina, VSX2 protein is not detected, and the *orJ* allele is considered a functional
70 null.[1,3,10] The other two alleles are gene targeted missense mutations that are
71 homologous to human variants associated with congenital microphthalmia and
72 blindness: a glutamine substitution for arginine at amino acid position 200 (*R200Q*;
73 MGI:5449355), and a tryptophan substitution of arginine at position 227 (*R227W*;
74 MGI:5449356; (Fig. 1A)).[3] Like the *orJ* allele, both are recessive, and their phenotypes
75 are consistent with disrupted *Vsx2* function although they differ in severity. The *R200Q*
76 mutant closely phenocopies *orJ,* while the *R227W* mutant is more severe as revealed
77 by even smaller eyes, increased pigmentation of the retina, and a failure to initiate
78 neurogenesis.[3] The *R200Q* and *R227W* alleles also differ from *orJ* in that the mutant
79 proteins are expressed.[3] The *R200Q* mutation is in the homeodomain and abrogates
80 DNA binding to canonical sites.[3,13] The *R227W* mutation is in the CVC domain, a
81 conserved stretch of approximately 50 amino acids that is a defining feature of the VSX
82 gene family.[3] Although its mechanism of action remains elusive, the CVC domain also
83 appears to promote DNA binding and sumoylation.[14,15] Consistent with its role in DNA
84 binding, the *R227W* protein exhibits weakened binding to canonical VSX2 binding
85 sites.[3]

86 Here, we expand the genetic toolkit for *Vsx2* with a new targeted allele that
87 replaces exon 3 with an IRES-*LacZ* expression cassette ($Vsx2^{LacZ}$). We show that b-
88 GAL protein expression from the *LacZ* cassette is a reliable reporter of endogenous

89 VSX2 expression, and that the ocular phenotype of the *Vsx2*^{LacZ} homozygous mutant
90 (*LacZ* mutant) exhibits the hallmarks of *Vsx2* disruption in a manner similar to the *orJ*
91 mutant. However, unlike *orJ*, the predicted truncated protein is expressed and there are
92 subtle differences in the *LacZ* mutant phenotype – leaving open the possibility that the
93 allele is not a complete knockout. This allele adds to the repertoire of *Vsx2* mutants in
94 which protein variants are expressed and provides an additional resource for probing
95 *Vsx2* function *in vivo*.
96

97 # Results

98 The VSX2-encoding portion of the *Vsx2*^{LacZ} mRNA is solely composed of exons 1
99 and 2, therefore lacking the homeodomain and CVC domain. This is followed by an
100 internal ribosome entry sequence (IRES) and *LacZ* cDNA, which encodes the
101 *Escherichia coli* b-GAL protein (Fig. 1A). The *Vsx2*^{LacZ} (*LacZ*) allele was generated by
102 Cre recombination of the *Vsx2*$^{tm1a(EUCOMM)Wtsi}$ allele (MGI ID:4453691),[16] and genomic
103 DNA PCR confirmed germline transmission (Fig. 1B). Western blot analysis of E15.5
104 retinal lysates probed with an antibody specific to the N-terminal portion of the human
105 VSX2 (aa1-131) revealed that like the *orJ* allele, full length VSX2 is not expressed from
106 the *LacZ* allele (Fig. 1C; top row). Unexpectedly, the predicted, truncated VSX2 protein
107 from the *LacZ* allele was detected, indicating stable expression (Fig. 1C; second row).
108 Detection of b-GAL confirmed that the gene targeting strategy was successful and that
109 the IRES was sufficient to produce two distinct proteins from the same transcript (Figure
110 1C; fourth row). Immunohistology revealed that the mutant protein lacked nuclear
111 localization, consistent with loss of the nuclear localization signal in exon 3 (Fig. 1D,E).

112 We also confirmed that b-GAL accurately reports VSX2 expression, indicated by their
113 extensive colocalization throughout development and easily visualized in the inner
114 nuclear layer (INL) of *LacZ* heterozygous retinas at P28. (Fig. 1F-I; Supplemental Fig.
115 1A-F). Finally, the stereotypical microphthalmic phenotype was evident and significant
116 at E12.5 (Fig. 1J-L).

117 We next performed immunohistology to characterize the *LacZ* mutant phenotype
118 in the retina. Establishment of optic cup regionalization appeared intact at E10.5 as
119 evidenced by VSX2 expression in the retina, LHX2 and PAX6 in the RPE and retina,
120 OTX1/2 and MITF in the RPE (Fig. 2A-E,G-K). The RPC and proliferation markers
121 PCNA and CCND1 also appeared to be normal in the E10.5 *LacZ* mutant retina
122 (Supplemental Fig. 2A-D). However, MITF was ectopically expressed in the retina (Fig.
123 2E,K) and PAX2 expression extended into the dorsal retina in the *LacZ* mutant (Fig.
124 2F,L; arrows). At E11.5, VSX2, LHX2, and PAX6 expression remained unaltered (Fig.
125 2M-O,S-U), but the ectopic expression of MITF (Fig. 2E,K) and dorsal expression of
126 Pax2 (Fig. 2R,X; arrows) were still evident, and OTX1/2 expression in the central retina
127 was elevated in the *LacZ* mutant (Fig. 2P,V). These altered expression patterns are
128 consistent with compromised retinal identity. Further evidence of altered retinal identity
129 was observed at E12.5 with continued ectopic expression of OTX1/2 in the peripheral
130 retina, most notably on the ventral side (Fig. 4E,K; arrows). From E11.5 to E15.5, the
131 RPC population, as indicated by PCNA, is maintained (Fig. 3A-F; Supplemental Fig.
132 2E,F), but proliferation progressively decreased, most notably in the peripheral retina,
133 as assessed by reduced CCND1 expression (Fig. 3G-L; Supplemental Fig. 2G,H;

134 arrows) and EdU incorporation (Fig. 3M-R; Supplemental Fig. 2I,J; arrows). This early
135 embryonic phenotype emulates those of the *orJ*, *R200Q,* and *R227W* mutants.[1,3]
136 Neurogenesis and establishment of the inner and outer neuroblastic layers
137 initiate at E11.5 in the central retina and progress out to the retinal peripheral margin by
138 E15.5. This is readily observed in the *LacZ* heterozygous retina at E12.5, E13.5, and
139 E15.5 using the expression of neurogenesis and cell-type specific markers including
140 TUBB3, a marker of cytoskeletal maturation in early post mitotic neuronal precursors,
141 ATOH7, a marker expressed by neurogenic progenitors preceding cell cycle exit,
142 BHLHB5 and POU4F2, markers of amacrine and RGCs respectively, and OTX1/2, a
143 marker of neurogenic RPCs biased towards photoreceptor fates as well as
144 photoreceptor precursors (Fig. 4A-E;M-Q; Supplemental Fig. 2K,M,O,Q,S). In contrast,
145 none of these neurogenesis markers were detected in the central retina of the *LacZ*
146 mutant at E12.5 (Fig. 4G-K). OTX1/2 was expressed in the peripheral ventral retina
147 (Fig. 4E,K; arrows), but as mentioned above, this expression is associated with
148 compromised retinal identity.[7] By E15.5 in the *LacZ* mutant, all markers were
149 expressed in patterns consistent with neurogenesis, although stained cells were
150 restricted to the central retina (Fig. 4S-W; arrows). Correlated with the delayed
151 neurogenesis is reduced expression of the neurogenic competence marker SOX2 at
152 E12.5 (Fig. 4F,L), and restricted expression in a small central region of the *LacZ* mutant
153 retina at E13.5 (Supplemental Fig.2 S,T; arrows) and E15.5 (Fig. 4R,X; arrows).[17]
154 These observations are consistent with a delay in the onset of retinal neurogenesis, to a
155 similar extent as the *orJ* and *R200Q* mutants.

156 We observed variation in the severity of the microphthalmic phenotype of *LacZ*
157 mutant embryos at E15.5, ranging from similar to more severe than in *orJ* embryos (Fig.
158 5A). Although the mean reduction in eye size of the *LacZ* and *orJ* mutants were similar
159 in magnitude when compared to their respective controls (Fig. 5B), variability was
160 greater in the *LacZ* mutants (Fig. 5C). We also observed variation in the extent of
161 neurogenesis, as assessed by TUBB3 expression, between *LacZ* mutants (Fig. 5D-G).
162 While neurogenic length and density were similar in the *LacZ* and *orJ* mutants (Fig.
163 5H,I; defined in methods), the extent of variation in these measurements were similar
164 except for neurogenic length in the *LacZ* mutants which was increased compared to the
165 other genotypes (Fig. 5J,K). Linear regression analysis revealed that neurogenic density
166 and eye size were highly correlated (Fig. 5L; $r^2 = 0.944$), but the correlation between
167 neurogenic length and eye size was weak (Fig. 5M; $r^2 = 0.364$). These observations
168 suggest a link between eye size and neuron production, but not between eye size and
169 progression of the neurogenic wave from the central to peripheral retina.
170 Given the variation in neurogenesis at E15.5, we hypothesized that differences
171 between the *LacZ* and *orJ* mutant phenotypes began earlier. We therefore focused on
172 the onset of neurogenesis, which exhibits a near stereotypical delay of two days in the
173 *orJ* retina, initiating at approximately E13.5.[8] Expression of TUBB3 (Fig. 5N; box and
174 inset) and OTX1/2 (Supplemental Fig. 2R; arrow) was observed at E13.5 in the central
175 retina of the *LacZ* mutant, but cells were sparse compared to the *LacZ* het
176 (Supplemental Fig. 2Q). Similarly, cells expressing the neurogenic progenitor marker
177 ATOH7 were present but sparse in the *LacZ* mutant retina (Supplemental Fig. 2K,L;
178 arrow), whereas POU4F2, and BHLHB5 were not detected (Supplemental Fig. 2M-P).

179 We therefore examined TUBB3 staining in retinas from the *LacZ* and *orJ* mutants at
180 E13.25. Indeed, neurogenesis was not observed at E13.25 in the *LacZ* mutant retina
181 (n=7) but was in the *orJ* mutant retina (n=4; Fig. 5O-Q). The sum of these observations
182 suggests that the *LacZ* mutant exhibits subtle increases in phenotypic severity
183 compared to the *orJ* mutant (see discussion).

184 Elevated MITF expression in the retina is a central driver of the *Vsx2* mutant
185 phenotypes, and a semi-dominant negative allele of *Mitf* (*Mitf*^{mi}) is sufficient to
186 significantly reduce phenotypic severity.[3,8,9,17] We predicted a similar outcome with the
187 *LacZ* allele, and to test this, we crossed *LacZ* mutant, *Vsx2*$^{Z/Z}$, mice with our *Vsx2*$^{orJ/orJ}$;
188 *MITF*$^{mi/+}$ line to generate *Vsx2*$^{orJ/Z}$; *MITF*$^{mi/+}$ embryos. At both E12.5 and E15.5,
189 *Vsx2*$^{orJ/Z}$; *MITF*$^{mi/+}$ eyes were significantly larger than those of *Vsx2*$^{orJ/Z}$; *MITF*$^{+/+}$ (Fig. 6).
190 This suggests that, like the other *Vsx2* mutants, *Mitf* has a prominent role in causing
191 microphthalmia in the *LacZ* mutant retina.

192 The effects of early *Vsx2* dysfunction are compounded in the postnatal retina as
193 seen by severe hypocellularity and tissue disorganization. Additionally, due to the
194 specific postnatal requirement of *Vsx2* for the specification and differentiation of the last
195 neuronal cell class, bipolar cells, they are not generated.[1,6,11,18] These features are also
196 evident in the *LacZ* mutant retina. At P0 (Fig. 7), the *LacZ* mutant retina is reduced to a
197 1-3 cell-thick, epithelium consisting of dispersed RPCs (EdU, MCM6, SOX9) and
198 differentiating retinal cells (TUBB3) including Müller glia (SOX9), RGC's (POU4F2),
199 amacrine cells (BHLHB5), and photoreceptors (RECOVERIN, OTX1/2). At P10 (Fig. 8),
200 the thin apical epithelium, composed largely of photoreceptors (RECOVERIN, OTX1/2)
201 remains intact while an additional population of disorganized aberrantly proliferating

202 RPCs (EdU, MCM6), and new neurons (TUBB3) including Müller glia (SOX9), RGCs
203 (POU4F2), and amacrine cells (BHLHB5) arises basal to the organized epithelium.
204 Signs of degeneration emerge at P14 (Supplemental Fig. 3), as the cellular organization
205 at the apical surface becomes disrupted and hypocellular regions, possibly plexiform
206 outgrowths, arise in the disorganized basal cell layer. By P28 (Fig. 9), the retina has
207 severely degenerated - consisting of disorganized retinal progenitor cells, and specified
208 Müller glia, RGCs, amacrine cells, and photoreceptors. Consistent with the other *Vsx2*
209 mutants, bipolar cells are not observed in the *LacZ* mutant retina at P14 (Supplemental
210 Fig. 3Q-T) or P28 (Fig. 10) as revealed by PKCα (PKC) and VSX1. Interestingly, sparse
211 PKC-positive cells were observed at P14, which could suggest some bipolar cell
212 formation, but this antibody also detects amacrine cells, which likely accounts for the
213 pattern observed P28.[6]
214

215 # Discussion

216 Based on the observations reported here, we propose that the *LacZ* allele
217 exhibits loss-of-function properties with strong phenotypic similarities to the *orJ* null
218 allele, which lacks protein expression, and the *R200Q* allele, which produces a DNA
219 binding-deficient protein.[3] All three mutants exhibit bilateral microphthalmia, reduced
220 retinal proliferation, delayed neurogenesis, an absence of bipolar cells, and are affected
221 by ectopic Mitf activity.[3,8,9,12,17] Because the mutant VSX2 protein is expressed, we
222 cannot conclude that the *LacZ* allele is a complete knockout, and consistent with this,
223 we observed subtle differences in the timing of neurogenesis onset in the *LacZ* mutant

224 retinas compared to *orJ* mutant, and greater variability amongst *LacZ* mutants at E15.5
225 when compared to that of *orJ* mutants in both eye size and parameters of neurogenesis.
226 There are two reasons that could account for these differences. One is that the
227 mutant protein is not inert (see below). The other is that the *LacZ* mutant phenotype is
228 sensitive to its genetic background, which has been documented for the *orJ* mutant
229 phenotype. The *orJ* mutation was discovered in the 129svimj background, but when
230 outcrossed, phenotypic variations occur.[5,11,19] For example, increased pigmentation
231 and more severe microphthalmia resulted when *orJ* mice were bred with mice with
232 mixed genetic backgrounds including C57Bl6 mice.[20] We also observed similar
233 increases in phenotypic severity in an outcross with Black Swiss mice (unpublished). In
234 contrast, less severe phenotypes were observed when *orJ* mice were crossed to
235 *p27Kip1* (*Cdkn1b*) knockout mice on a C57BL/6 genetic background[6] or outcrossed with
236 wild type *Mus castaneous*.[11] Relevant here is that our characterization of the *LacZ*
237 allele was done in a mixed C57BL/6;129sv mixed genetic background which could
238 contribute to variations in phenotypic severity.
239 It is also possible that the mutant VSX2 protein has activity, but what this activity
240 might be is not clear. The mutant coding sequence extends from amino acid 1 through
241 151 (out of 361 or 380; https://www.ncbi.nlm.nih.gov/protein/NP_031727) and lacks the
242 homeodomain and CVC domain, making direct DNA binding unlikely. Interactions with
243 other proteins are possible, but domains or motifs have not been identified in the
244 retained N-terminal portion of VSX2 other than putative disordered regions**.** It is also
245 possible that the mutant protein has novel or neomorphic activity because it is no longer
246 localized to the nucleus, but how this might alter the phenotype is hard to reconcile

247 because the allele is not dominant. Interestingly, the *R227W* allele exhibits properties of
248 a recessive neomorph.[3] We attributed this to the ability of the *R227W* mutant protein to
249 activate a cryptic transcriptional circuit that increased non-retinal gene expression,
250 including *Mitf,* beyond that observed in the *orJ* mutant retina.[3] Further work is needed
251 to determine if the truncated VSX2 protein from the *LacZ* allele has activity.
252 In summary, the *LacZ* allele is a new addition to the allelic series of *Vsx2*
253 mutations, and its functional properties make it useful for further probing *Vsx2* function
254 in the *in vivo* context.
255

256 # Experimental Procedures

257 ## *Animals*

258 The $Vsx2^{LacZ}$ line was generated from ES cells containing the $Vsx2^{tm1a(EUCOMM)Wtsi}$
259 allele. Germline founders were crossed with CMV-Cre mice (RRID:IMSR_JAX:006054)
260 to excise the *LoxP* flanked region containing the Neo cassette and *Vsx2* exon 3 to
261 create the $Vsx2^{LacZ}$ strain. $Vsx2^{orJ}$ mice (RRID:IMSR_JAX:000395) and $Mitf^{mi}$ mice
262 (RRID:IMSR_JAX001573) are maintained in the laboratory.

263 ## *Tissue collection*

264 Embryos and pups were generated using single night matings, with the day that
265 the vaginal plug was observed considered E0.5. $Vsx2^{LacZ}$ embryos were collected at
266 E10.5, E11.5, E12.5, E13.5, E15.5 and $Vsx2^{LacZ}$ pups were collected at P0, P10, P14,
267 and P28. All embryos and pups were staged using whole-body attributes.[21–23]
268 EdU was administered via IP injection – for embryos, the dam was treated 2
269 hours before dissection, while the postnatal pups were injected 45 minutes before

270 dissection. Dams were euthanized using CO_2 and cervical dislocation, while pups were
271 anesthetized using hypothermia and thereafter euthanized via decapitation. At E15.5,
272 embryo eyelids were removed for imaging to allow for accurate eye size quantification.

273 ***Tissue preparation***

274 Embryo heads and postnatal pup eyes were fixed at room temperature in 4%
275 PFA-PBS solution for 45 minutes or 1 hour, respectively. After several PBS washes, a
276 sucrose cryopreservation series was performed before the samples were frozen in
277 TissueTek OCT (Sakura Finetech) and stored at -80°C. Tissue was sectioned in twelve
278 micrometer sections at -20°C with a Leica CM1950 cryostat and adhered to Superfrost
279 Plus slides (Fisher Scientific). The sections were then dried for 1-2 hours before storage
280 at -20°C and -80°C.

281 ***Western Blot***

282 Freshly dissected E15.5 retinal tissue was flash frozen in liquid nitrogen and
283 stored at -80°C. Lysates were prepared with RIPA buffer at a volume of 100 µL per 50
284 mg of tissue. Lysates for heterozygotes contained 2 retinas per sample (1 animal) and 4
285 retinas per sample (2 animals) for homozygotes. BCA assay (Quick Start Bradford, Bio
286 rad) was used to determine protein concentration using a wavelength of 595 nm. 20 ug
287 of protein per lane was loaded in a 20 µL volume. Gels were run for 40 min at 90 V and
288 then 40 min at 110 V. Proteins were transferred using an iblot2 (Fisher Scientific)
289 system with a setting of 15V in 7 mins. Blots were blocked for 1 hour at room
290 temperature using 5% BSA in 1X PBST buffer. Primary antibodies were diluted in 1X
291 PBST and blots were exposed to primary antibodies overnight at 4°C. Blots were
292 washed 3 times for 10 minutes using 5% BSA in PBST, then exposed to secondary

293 antibody for 1 hour at room temperature. Washed 6 times for 10 minutes using PBST.
294 Chemiluminescence HRP substrate (Immobilon Western, Millipore) was used for signal
295 detection and images were captured on an Amersham Imager 600 (General Electric).

296 ***Immunohistochemistry***

297 To remove OCT, slides were washed in PBS, and incubated in block solution
298 (2% donkey serum, 0.1% triton-x100, PBS pH 7.4) for 60 minutes at room temperature.
299 Slides were then incubated in primary antibody solution overnight at 4°C. Primary
300 antibody solution was removed and several PBST washes performed before the slides
301 were incubated in secondary antibodies at room temperature for an hour in a dark
302 humidified chamber. Additional PBST washes were performed, EdU incorporation was
303 detected using AlexaFluor 568 or 647 Click-iT Cell Reaction Kit (Invitrogen-Molecular
304 Probes, Eugene, Oregon) and a DAPI (1:40000 in PBS) solution was applied for 10
305 minutes. The slides were then dried and coverslipped with Fluoromount and stored at
306 4°C until imaging.

307 ***Quantifications and Statistics***

308 Eye size was quantified using the pentagon-ROI tool of Fiji on embryo pictures
309 taken on a Nikon C-FIDH SMZ1270. Eye size was defined by the area of the two-
310 dimensional circumference of the pigmented eye (sphere). Area was measured in
311 pixels^2 and converted to μm^2. Neurogenic length, as defined by the linear length of the
312 retinal basal surface that TUBB3-positive cells occupy, was quantified using the
313 freehand line-ROI tool of Fiji and the percentage calculated by dividing the neurogenic
314 length by the total length of the retinal basal surface and multiplying by 100. Neurogenic
315 density, as defined by the number of TUBB3-positive pixels divided by the total number

316 of pixels in the neurogenic region (the apicobasal region of the retina containing
317 TUBB3-positive cells), is used as a proxy for cells within the neurogenic region. This
318 was quantified using Fiji by creating an ROI outlining the TUBB3-positive region of the
319 retina and clearing the non-ROI regions using Edit>Clear Outside. The neurogenic
320 region was then made binary using Threshold tool, then the number of positive (white)
321 and negative (black) pixels were quantified using Analyze>Histogram. The neurogenic
322 density was then calculated using the ratio of positive pixels to total pixels in the
323 neurogenic region. Prism was used to run t-tests, one-way ANOVAs, post-hoc analyses,
324 to assess statistical significance, and to create graphical representations.

325 ***Imaging/Microscopy***

326 Whole embryos were imaged using Nikon C-FIDH SMZ1270. Immunofluorescent
327 staining at E10.5-E11.5 and postnatal stages were imaged using a Nikon Eclipse E600
328 while those at E12.5-E15.5 were imaged using a Zeiss LSM710 confocal microscope
329 with 20X lens to capture a high-resolution image of the relatively larger ROI. Image
330 histograms were adjusted using Fiji. Images were resized and trimmed using Adobe
331 Photoshop. Figures were made using Adobe Illustrator.

332

333

334 Acknowledgments

335 Funding was provided by the National Eye Institute (R01-EY013760; P30-EY008126)
336 and an unrestricted grant from Research to Prevent Blindness, Inc. AAH was supported
337 by the National Science Foundation Graduate Research Fellows Program (1937963).
338 The Zeiss LSM710 confocal microscope used for this study was acquired with funding

from NIH (S10-RR027396). We thank members of the Levine and Fuhrmann laboratories for their insights and feedback.

Ethics Statement

All procedures and experiments with mice were approved by the Vanderbilt Institutional Animal Care and Use Committee and conformed to the ARVO guidelines for the use of animals in vision research. The research was conducted in concordance with the NIH guidelines for Responsible Conduct in Research.

Disclosure

The authors report no conflicts of interest in this work.

351 # References

352

353 1. Burmeister M, Novak J, Liang MY, et al. Ocular retardation mouse caused by Chx10
354 homeobox null allele: impaired retinal progenitor proliferation and bipolar cell
355 differentiation. *Nat Genet*. 1996;12(4):376-384. doi:10.1038/ng0496-376

356 2. Liu ISC, Chen J de, Ploder L, et al. Developmental expression of a novel murine
357 homeobox gene (Chx10): Evidence for roles in determination of the neuroretina and
358 inner nuclear layer. *Neuron*. 1994;13(2):377-393. doi:10.1016/0896-6273(94)90354-9

359 3. Zou C, Levine EM. Vsx2 Controls Eye Organogenesis and Retinal Progenitor Identity
360 Via Homeodomain and Non-Homeodomain Residues Required for High Affinity DNA
361 Binding. *Plos Genet*. 2012;8(9):e1002924. doi:10.1371/journal.pgen.1002924

362 4. Phillips MJ, Perez ET, Martin JM, et al. Modeling human retinal development with
363 patient-specific iPS cells reveals multiple roles for VSX2. *Stem Cells*. Published
364 online 2014:n/a-n/a. doi:10.1002/stem.1667

365 5. Theiler K, Varnum DS, Nadeau JH, Stevens LC, Cagianut B. A new allele of ocular
366 retardation: early development and morphogenetic cell death. *Anat Embryol*.
367 1976;150(1):85-97. doi:10.1007/bf00346288

368 6. Green ES, Stubbs JL, Levine EM. Genetic rescue of cell number in a mouse model of
369 microphthalmia: interactions between Chx10 and G1-phase cell cycle regulators.
370 *Development*. 2003;130(3):539-552. doi:10.1242/dev.00275

371 7. Sigulinsky CL, German ML, Leung AM, Clark AM, Yun S, Levine EM. Genetic
372 chimeras reveal the autonomy requirements for Vsx2 in embryonic retinal progenitor
373 cells. *Neural Dev*. 2015;10(1):12. doi:10.1186/s13064-015-0039-5

374 8. Leung AM, Rao MB, Raju N, et al. A framework to identify functional interactors that
375 contribute to disrupted early retinal development in Vsx2 ocular retardation J mice.
376 *Dev Dyn*. Published online 2023. doi:10.1002/dvdy.629

377 9. Horsford DJ, Nguyen MTT, Sellar GC, Kothary R, Arnheiter H, McInnes RR. Chx10
378 repression of Mitf is required for the maintenance of mammalian neuroretinal identity.
379 *Development*. 2005;132(1):177-187. doi:10.1242/dev.01571

380 10. Rowan S, Chen CMAM, Young TL, Fisher DE, Cepko CL. Transdifferentiation of the
381 retina into pigmented cells in ocular retardation mice defines a new function of the
382 homeodomain gene Chx10. *Development*. 2004;131(20). doi:10.1242/dev.01300

383 11. Bone-Larson C, Basu S, Radel JD, et al. Partial rescue of the ocular retardation
384 phenotype by genetic modifiers. *J Neurobiol*. 2000;42(2):232-247.
385 doi:10.1002/(sici)1097-4695(20000205)42:2<232::aid-neu7>3.0.co;2-4

386 12. Bharti K, Liu W, Csermely T, Bertuzzi S, Arnheiter H. Alternative promoter use in
387 eye development: the complex role and regulation of the transcription factor MITF.
388 *Development*. 2008;135(6):1169-1178. doi:10.1242/dev.014142

389 13. Percin EF, Ploder LA, Yu JJ, et al. Human microphthalmia associated with
390 mutations in the retinal homeobox gene CHX10. *Nat Genet*. 2000;25(4):397-401.
391 doi:10.1038/78071

392 14. Kurtzman AL, Schechter N. Ubc9 interacts with a nuclear localization signal and
393 mediates nuclear localization of the paired-like homeobox protein Vsx-1
394 independent of SUMO-1 modification. *Proc Natl Acad Sci USA*. 2001;98(10):5602-
395 5607. doi:10.1073/pnas.101129698

396 15. Dorval KM, Bobechko BP, Ahmad KF, Bremner R. Transcriptional activity of the
397 paired-like homeodomain proteins CHX10 and VSX1. *J Biol Chem*.
398 2005;280(11):10100-10108. doi:10.1074/jbc.m412676200

399 16. Skarnes WC, Rosen B, West AP, et al. A conditional knockout resource for the
400 genome-wide study of mouse gene function. *Nature*. 2011;474(7351):337-342.
401 doi:10.1038/nature10163

402 17. Konyukhov B, Sazhina M. Interaction of the genes of ocular retardation and
403 microphthalmia in mice. *Folia Biol (Praha)*. 1966;12(2):116-123.
404 http://eutils.ncbi.nlm.nih.gov/entrez/eutils/elink.fcgi?dbfrom=pubmed&id=4958088&r
405 etmode=ref&cmd=prlinks

406 18. Goodson NB, Kaufman MA, Park KU, Brzezinski JA. Simultaneous deletion of
407 Prdm1 and Vsx2 enhancers in the retina alters photoreceptor and bipolar cell fate
408 specification, yet differs from deleting both genes. *Development*.
409 2020;147(13):dev190272. doi:10.1242/dev.190272

410 19. Wong G, Conger SB, Burmeister M. Mapping of genetic modifiers affecting the eye
411 phenotype of ocular retardation (Chx10or-J) mice. *Mamm Genome*.
412 2006;17(6):518-525. doi:10.1007/s00335-005-0159-z

413 20. Rowan S, Cepko CL. Genetic analysis of the homeodomain transcription factor
414 Chx10 in the retina using a novel multifunctional BAC transgenic mouse reporter.
415 *Dev Biol*. 2004;271(2):388-402. doi:10.1016/j.ydbio.2004.03.039

416 21. Wong MD, Eede MC van, Spring S, et al. 4D atlas of the mouse embryo for precise
417 morphological staging. *Development*. 2015;142(20):3583-3591.
418 doi:10.1242/dev.125872

419 22. Theiler K. *The House Mouse: Atlas of Embryonic Development*. Springer, Berlin;
420 1989. doi:10.1007/978-3-642-88418-4

421 23. Kaufman MH. *The Atlas of Mouse Development*. Elsevier Science; 1992.
422 https://books.google.com/books?id=Lo5pAAAAMAAJ

423

424

425 **Table 1: Primary antibodies**

NAME	SPECIES[1]	DILUTION[2]	SOURCE	CATALOG #	RRID
ATOH7	Rb	1:200 (IH)	Novus Biologicals	NBP1-88639	AB_11034390
b-GAL	Ms	1:200 (IH) 1:1000 (WB)	Developmental Studies Hybridoma Bank	40-1a-s	AB_528100
BHLHB5	Rb	1:200 (IH)	Santa Cruz Biotechnology	sc-6045	AB_2065343
CCND1	Rb	1:400 (IH)	Abcam	ab16663 (SP4)	AB_443423
LHX2	Rb	1:300 (IH)	GeneTex	GTX129241	AB_2783558
MCM6	Gt	1:300 (IH)	Santa Cruz Biotechnology	sc-9843	AB_2142543
MITF	Ms	1:800 (IH)	Exalpha Biologicals Inc.	X1405M	-
OTX1/2	Gt	1:1000 (IH)	GeneTex	AF1979	AB_2157172
PAX2	Rb	1:100 (IH)	Covance Laboratories	PRB-276P	AB_291611
PAX6	Rb	1:300 (IH)	BioLegend	901301	AB_2565003
PCNA	Ms	1:500 (IH)	Santa Cruz Biotechnology	sc-56	AB_628110
PKC	Rb	1:200 (IH)	Sigma-Aldrich	P-4334	AB_477345
POU4F2	Gt	1:200 (IH)	Santa Cruz Biotechnology	sc-6026	AB_673441
RECOVERIN	Rb	1:100 (IH)	Chemicon International	AB5585	AB_2253622
SOX2	Rb	1:400 (IH)	Abcam	ab97959	AB_2341193
SOX9	Rb	1:1000 (IH)	EMD Serono Inc	AB5535	AB_2239761
TUBB3	Rb	1:40K (IH)	BioLegend	802001	AB_2564645
VSX1	Rb	1:250 (IH)	Levine Lab	-	-
VSX2 - NT	Sh	1:400 (IH) 1:1000 (WB)	Exalpha Biologicals Inc.	X1180P	AB_2314191
ATP5A1	Rb	1:2000 (WB)	Proteintech	14676-1-AP	

[1] Gt, goat; Ms, mouse; Rb, rabbit; Sh, sheep
[2] IH, immunohistology; WB, western blot

426

427 **Abbreviations:**

428 b-GAL, beta-Galactosidase; C, cornea; CM, ciliary margin; D, dorsal; E, embryonic;

429 EdU, 5-Ethynyl-2'-deoxyuridine; GCL, ganglion cell layer; het, heterozygous; INL, inner

430 nuclear layer; IRES, internal ribosome entry sequence; LacZ, *Escherichia coli* lacz

431 gene; L, lens; *orJ*, *ocular retardation J*; ONL, outer nuclear layer; P, postnatal; R, retina;

432 RGC, retinal ganglion cell; RPC, retinal progenitor cell; RPE, retinal pigmented
433 epithelium; V, ventral.
434
435
436 **Figure Legends**
437 **Figure 1. *Vsx2^{LacZ}* recombination confirmation and gross phenotype. (A)**
438 Schematic of *Vsx2^{LacZ}* allele and resultant mRNA following Cre recombination. **(B)**
439 Genomic DNA PCR shows mendelian inheritance of *Vsx2* wildtype and *LacZ*
440 sequences confirming germline transmission. **(C)** Western blot analysis of E15.5 retinal
441 lysates. The N-terminal specific VSX2 antibody was used in the top 2 rows to detect full
442 length and truncated VSX2 proteins. B-GAL antibody was used in 4th row to detect b-
443 GAL expression from *LacZ allele*. Vsx2 and b-GAL antibodies were used on separate
444 blot. The probing for ATP5A1 serves as a loading control for each blot. **(D-E)**
445 Immunohistology at E15.5 reveals continued yet differentially localized expression of
446 VSX2 in the *LacZ* mutant (retinas are contained within the dashed lines) **(F-I)**
447 Recombination reporter, b-GAL, is co-expressed with VSX2 in the *LacZ* heterozygote at
448 P28. **(J-L)** Microphthalmia phenotype of the *LacZ* mutant is observable and significant
449 at E12.5. Abbreviations: ONL, outer nuclear layer; INL, inner nuclear layer; GCL,
450 ganglion cell layer. Scale bars: (D-H) 100 μm; (J,K) 2000 μm.
451
452 **Figure 2. Regionalization of the early embryonic *LacZ* mutant eye. (A-L)** Markers of
453 eye field specification and regionalization at E10.5. All markers exhibit similar
454 expression patterns in the *LacZ* mutant compared to the *LacZ* het except for MITF,

455 which is ectopically expressed in the retina (E,K) and PAX2, which is expanded into the
456 dorsal retina (arrows; F,L). **(M-X)** Markers of eye field specification and regionalization
457 at E11.5. MITF continues to be ectopically expressed (Q,W) and PAX2 extends into the
458 dorsal retina of the *LacZ* mutants (arrows; R,X). All other markers were similar between
459 the *LacZ* het and mutant. Abbreviations: R, retina; RPE, retinal pigment epithelium; CM,
460 ciliary margin; L, lens; C, cornea. Scale bar: 100 μm.
461
462 **Figure 3. Proliferation is reduced in the embryonic *LacZ* mutant retina. (A-F)** The
463 general proliferation marker PCNA remains expressed throughout the *LacZ* mutant
464 retina, similar to the *LacZ* het at E11.5, E12.5, and E15.5. In contrast, the patterns of
465 CCND1 expression **(G-L)** and EdU incorporation **(M-R)** became progressively restricted
466 to the central retina in the *LacZ* mutants compared to *LacZ* hets, most notably at E12.5
467 and E15.5. Arrows in I-L and O-R point to the regions where staining is absent in the
468 LacZ mutant retina compared to the *LacZ* het. Scale bar: 100 μm.
469
470 **Figure 4. Retinal neurogenesis is delayed and centrally restricted in the *LacZ***
471 **mutant.** Immunohistology assessing cytoskeletal maturation with TUBB3 **(A,G,M,S)**, the
472 presence of neurogenic progenitors with ATOH7 **(B,H,N,T)**, retinal ganglion cells with
473 POU4F2 **(C,I,O,U)**, amacrine cells with BHLHB5 **(D,J,P,V)** and photoreceptor
474 precursors with OTX1/2 (**E,K,Q,W)**, reveal a delay in neurogenesis in the *LacZ* mutant
475 retina, with markers lacking at E12.5 and centrally restricted at E15.5 (arrows in S-W).
476 OTX1/2 staining also reveals ectopic staining in the ventral peripheral retina at E12.5
477 (compare red arrows in E and K), which is associated with compromised retinal identity.

478 Expression of neurogenic competence regulator SOX2 in RPCs is reduced at E12.5
479 (F,L) and centrally restricted at E15.5 in the *LacZ* mutant retina (R,X; arrow denotes
480 region of persistent SOX2 expression). Scale bar: 100 μm.
481
482 **Figure 5. Timing of neurogenesis initiation and E15.5 variation in *LacZ* mutant**
483 **deviate from the *orJ* mutant phenotype. (A)** Microphthalmia was similar in the *LacZ*
484 and *orJ* mutants at E15.5, but severity was variable in the *LacZ* mutants (compare iii
485 and iv). **(B,C)**. Quantifications of eye size revealed similar degrees of severity (B), but
486 the coefficient of variation (CV) was highest in the *LacZ* mutants compared to the other
487 genotypes **(D-G)** TUBB3 expression, indicating neurogenesis, is centrally restricted and
488 seemingly covaries with microphthalmia severity in *LacZ* mutant at E15.5. **(H,I)**
489 Neurogenic density (H) and length (I) are similarly decreased in the *LacZ* and *orJ*
490 mutants. **(J,K)** Coefficients of variation (CV) for neurogenic density were similar across
491 genotypes (J; *LacZ* and *orJ* hets were combined), but the CV for neurogenic length was
492 specifically increased in the *LacZ* mutant. **(L)** Linear regression analysis of eye size and
493 neurogenic density in *LacZ* mutant retinas at E15.5. **(M)** Linear regression analysis of
494 eye size and neurogenic length in *LacZ* mutant retinas at E15.5. **(N-Q)** Neurogenesis
495 initiates at E13.5 in *LacZ* mutant (compare N to P). In contrast, neurogenesis initiates in
496 the *orJ* retina by E13.25 (Q). Scale bars: (A) 500 μm; (D-G; N-Q) 100 μm.
497
498 **Figure 6. Functional rescue of embryonic *LacZ* mutant microphthalmic phenotype**
499 **with *Mitf*$^{mi/+}$ allele.** The semi-dominant negative allele *MITF*$^{mi/+}$ reduced the severity of

500 microphthalmia in *Vsx2*$^{orJ/Z}$ mutants at E12.5 **(A-C)** and E15.5 **(D-F)**. Scale bar: 1000
501 µm.
502
503 **Figure 7**. **Immunohistology at P0.** The *LacZ* mutant retina at P0 is reduced to a thin
504 epithelium, containing interspersed **(A-D,G,H)** proliferating RPCs (EdU, MCM6, SOX9).
505 **(E-P)** Similarly, markers of differentiating cells (TUBB3, POU4F2, BHLHB5, OTX1/2,
506 RECOVERIN are expressed in a disorganized manner. In addition to marking RPCs,
507 SOX9 could indicate precocious Müller glia differentiation. Scale bar: 100 µm
508
509 **Figure 8. Immunohistology at P10. (A-L)** A disorganized population of proliferating
510 cells (EdU, MCM6), new neurons (TUBB3, POU4F2, BHLHB5), and Müller glia (SOX9),
511 persist in the *LacZ* mutant retina. (**M-P)** In contrast, the photoreceptor markers OTX1/2
512 and RECOVERIN suggest the presence of an organized apical epithelium. Scale bar:
513 100 µm
514
515 **Figure 9. Immunohistology at P28.** The *LacZ* mutant retina at P28 is severely
516 degenerated and disorganized. Lacking cellular organization, spherical **(A-D)** aberrantly
517 proliferating cells are interspersed with **(E-P)** progenitors (MCM6, SOX9), differentiating
518 neuronal cells (TUBB3), Müller glia (SOX9), retinal ganglion cells (POU4F2), amacrine
519 cells (BHLHB5), and photoreceptors (OTX1/2, RECOVERIN). Scale bar: 100 µm
520
521 **Figure 10. Bipolar cells are not detected in the *LacZ* mutant retina. (A-D)** The rod-
522 bipolar marker PKC is not detected in the *LacZ* mutant retina at P10, but basally

523 displaced cells are observed at P28. This antibody also detects amacrine cells at this
524 age. **(E,F)** The cone-bipolar marker VSX1 is not detected in the *LacZ* mutant retina at
525 P10 or P28. Scale bar: 100 μm
526
527 **Supplemental Figure 1. Expression of VSX2 and b-GAL in postnatal *LacZ***
528 **heterozygous retina. (A,B)** Immunohistology reveals b-GAL to be an accurate reporter
529 of VSX2 expression with both expressed throughout the *LacZ* heterozygous retina at
530 P0. **(C-F)** At P10 and P14, VSX2 and b-GAL are restricted to the INL, consistent with
531 expression in bipolar cells and Müller glia. All VSX2 and b-GAL stains are from the
532 same animal for each respective stage and genotype. Scale bar: 100 μm.
533
534 **Supplemental Figure 2. Immunohistology at E10.5 and E13.5. (A-D)** Expression of
535 the proliferation markers PCNA, CCND1, and pHH3 in the *LacZ* mutant retina are
536 normal at E10.5. **(E-J)** At E13.5, PCNA extends throughout the *LacZ* mutant retina
537 (E,F), whereas CCND1 are EdU) are limited to the central retina (G-J). Arrows in G-J
538 point to areas where staining is absent in the *LacZ* mutant compared to the *LacZ* het.
539 **(K,L)** ATOH7 expression is detected in a few cells in the central retina of the *LacZ*
540 mutant (arrow). **(M-P)** Retinal ganglion cells (POU4F2) and amacrine cells (BHLHB5)
541 are not detected in the *LacZ* mutant retina at E13.5. **(Q,R)** OTX1/2 expression is
542 detected in a few cells in the central retina of the *LacZ* mutant (arrow) **(S,T)** SOX2
543 expression is reduced in the peripheral retina of the *LacZ* mutant. Arrows in S and T
544 point to areas where staining is absent in the *LacZ* mutant compared to the *LacZ* het.
545 Scale bars: 100 μm.

546

547 **Supplemental Figure 3. *LacZ* mutant retina at P14. (A-F)** As the P14 retina continues
548 to aberrantly proliferate (EdU, MCM6) and give rise to new neurons (TUBB3), signs of
549 degeneration emerge. **(C-P)** The previously organized apical epithelium composed
550 largely of progenitors (MCM6, SOX9), Müller glia (SOX9), and photoreceptors (OTX1/2,
551 RECOVERIN) begins to seemingly lose its integrity as amongst the disorganized basal
552 cell population, consisting of progenitors (MCM6, SOX9), Müller glia (SOX9), retinal
553 ganglion cells (POU4F2) and amacrine cells (BHLHB5), hypocellular regions, possibly
554 plexiform outgrowths, encroach. **(Q,R)** PKC expressing cells are present in the *LacZ*
555 mutant retina, but their identity is not known, with possibilities being amacrine cells or
556 remnant bipolar cells. **(S,T)** VSX1 expressing cells are not detected in the *LacZ* mutant
557 retina. Scale Bar: 100 μm

558

559 **Supplemental Figure 4. Uncropped images for western blots in Figure 1C. (A)** Blot
560 1 probed with N-terminal VSX2 antibody, which detects the full length (VSX2 WT) and
561 truncated (VSX2 Mut) proteins. The last 4 lanes in panel A were used for the first two
562 rows in Fig. 1C. **(B)** Blot 1 stripped and re-probed with antibody to a validated reference
563 protein ATP5A1. The last 4 lanes in panel B were used for the third row in Fig. 1C. **(C)**
564 Blot 2 probed with b-GAL antibody. Spacings between lanes were cropped and the
565 bands at 100 kDa correspond to the fourth row in Fig. 1C. **(D)** Blot 2 was stripped and
566 reprobed with ATP5A1 antibody. Spacings between lanes were cropped and the bands
567 at 50 kDa correspond to the fifth row in Fig. 1C.

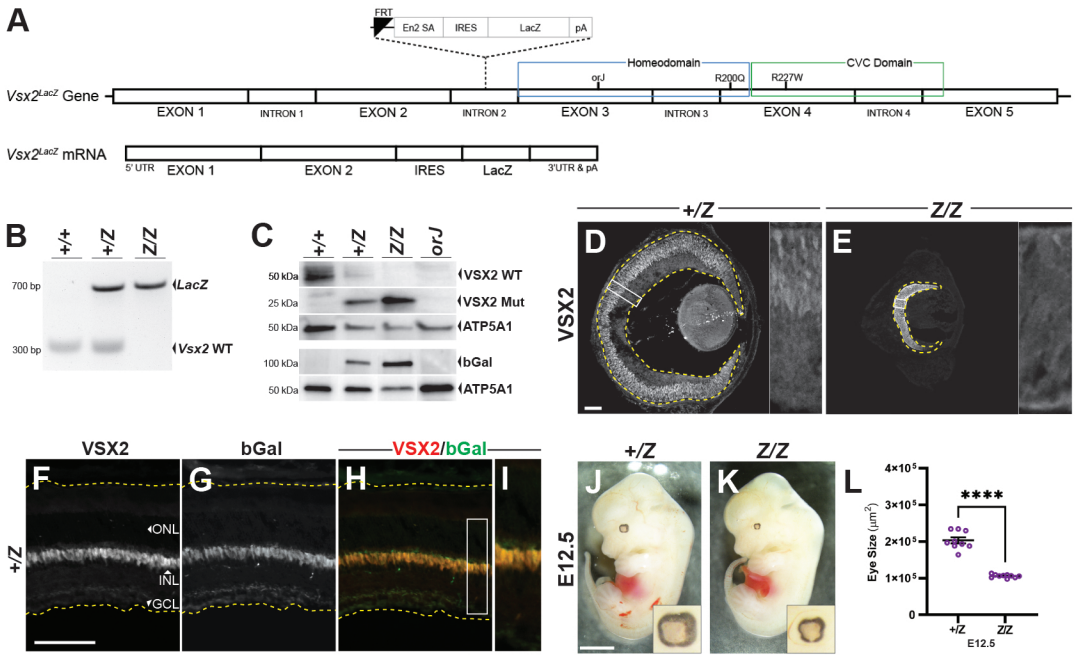
A
FRT
En2 SA
IRES
LacZ
pA
Homeodomain
CVC Domain
orJ
R200Q
R227W
Vsx2LacZ Gene
EXON 1
INTRON 1
EXON 2
INTRON 2
EXON 3
INTRON 3
EXON 4
INTRON 4
EXON 5
Vsx2LacZ mRNA
5' UTR
EXON 1
EXON 2
IRES
LacZ
3'UTR & pA
B
+/+
+/Z
Z/Z
700 bp
300 bp
LacZ
Vsx2 WT
C
+/+
+/Z
Z/Z
orJ
50 kDa
25 kDa
50 kDa
100 kDa
50 kDa
VSX2 WT
VSX2 Mut
ATP5A1
bGal
ATP5A1
+/Z
Z/Z
D
E
VSX2
VSX2
bGal
VSX2/bGal
F
G
H
I
+/Z
ONL
INL
GCL
+/Z
Z/Z
E12.5
J
K
L
4×10^5
3×10^5
2×10^5
1×10^5
0
Eye Size (μm^2)
****
+/Z
Z/Z
E12.5

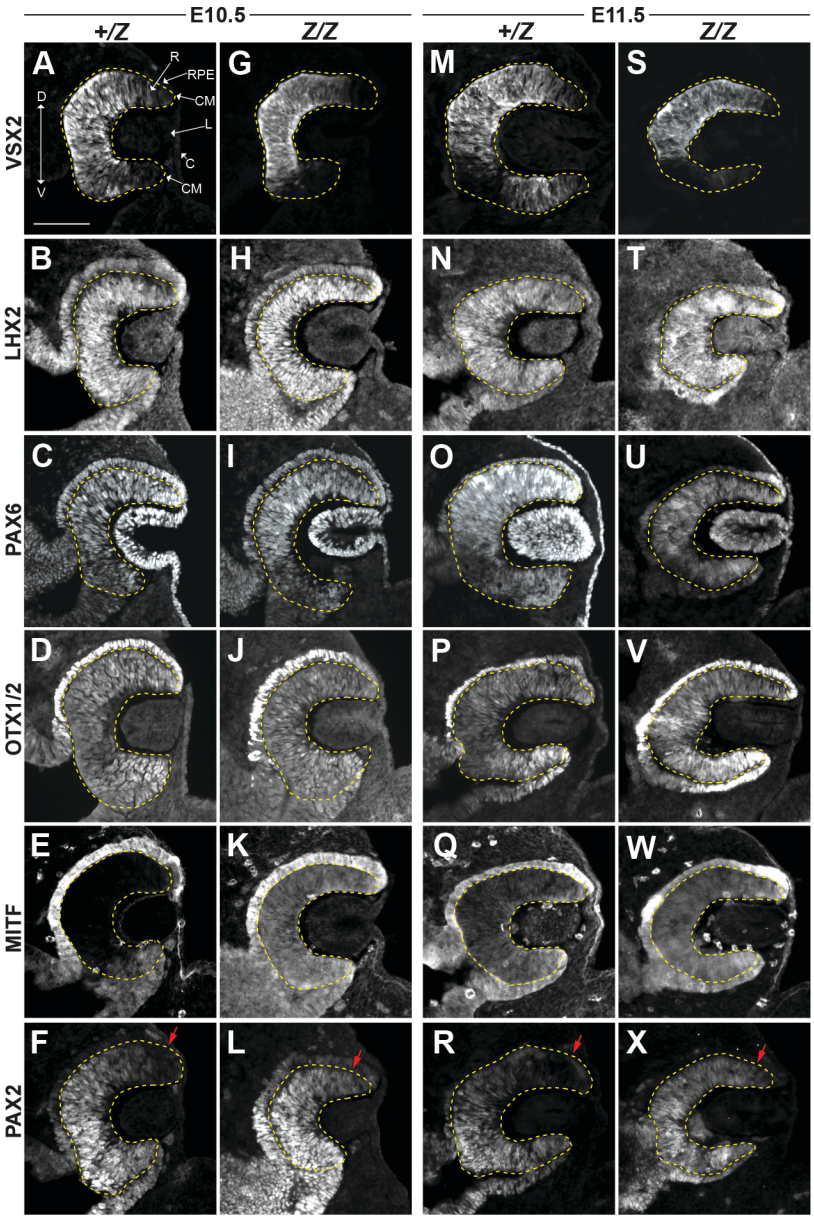
E10.5
E11.5
+/Z
Z/Z
+/Z
Z/Z
VSX2
LHX2
PAX6
OTX1/2
MITF
PAX2
A
B
C
D
E
F
G
H
I
J
K
L
M
N
O
P
Q
R
S
T
U
V
W
X
R
RPE
CM
L
C
CM
D
V

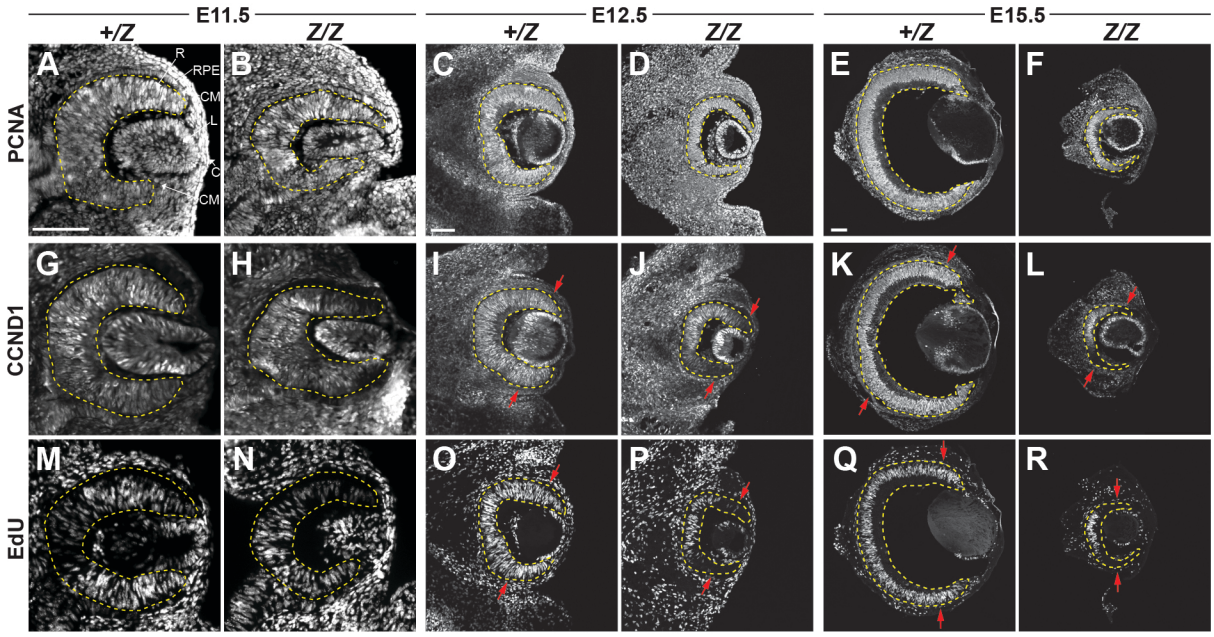
E11.5
E12.5
E15.5
+/Z
Z/Z
+/Z
Z/Z
+/Z
Z/Z
PCNA
CCND1
EdU
A
B
C
D
E
F
G
H
I
J
K
L
M
N
O
P
Q
R
R
RPE
CM
IL
C
CM

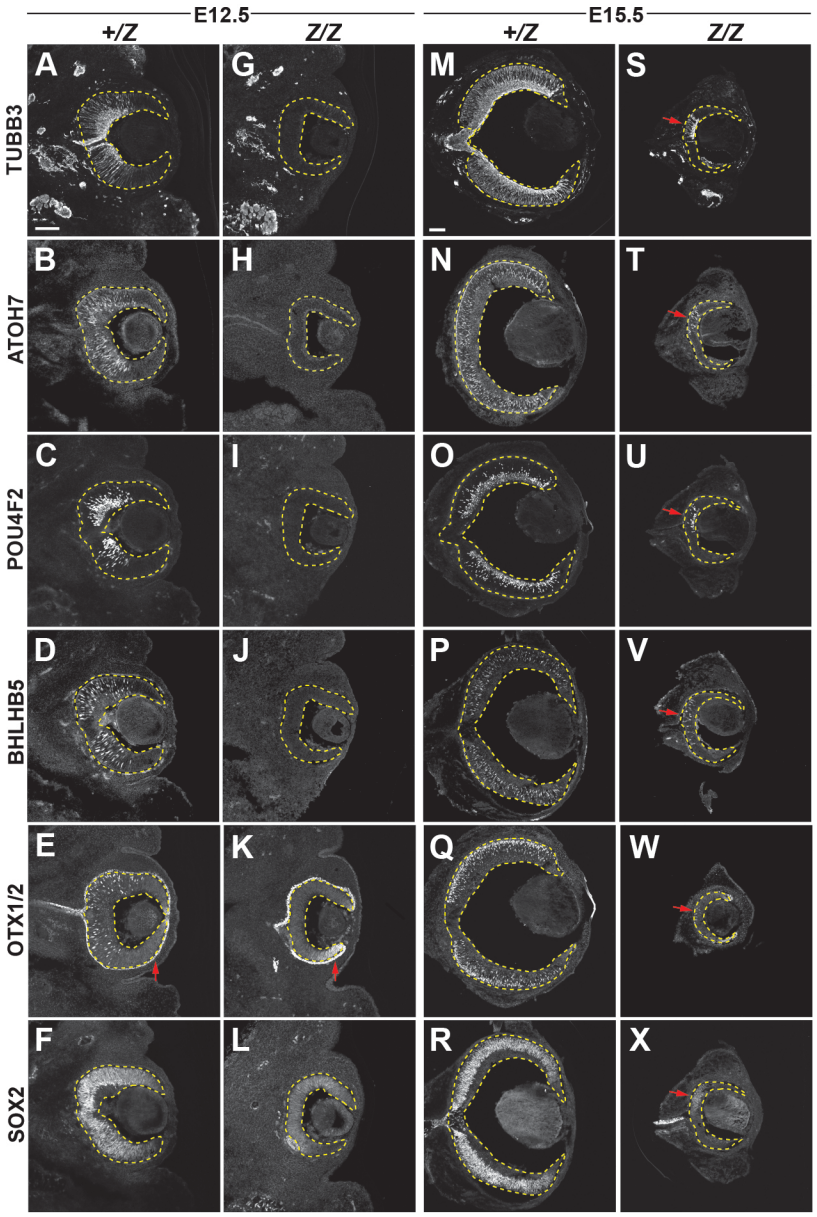
E12.5
E15.5
+/Z
Z/Z
+/Z
Z/Z
TUBB3
ATOH7
POU4F2
BHLHB5
OTX1/2
SOX2
A
G
M
S
B
H
N
T
C
I
O
U
D
J
P
V
E
K
Q
W
F
L
R
X

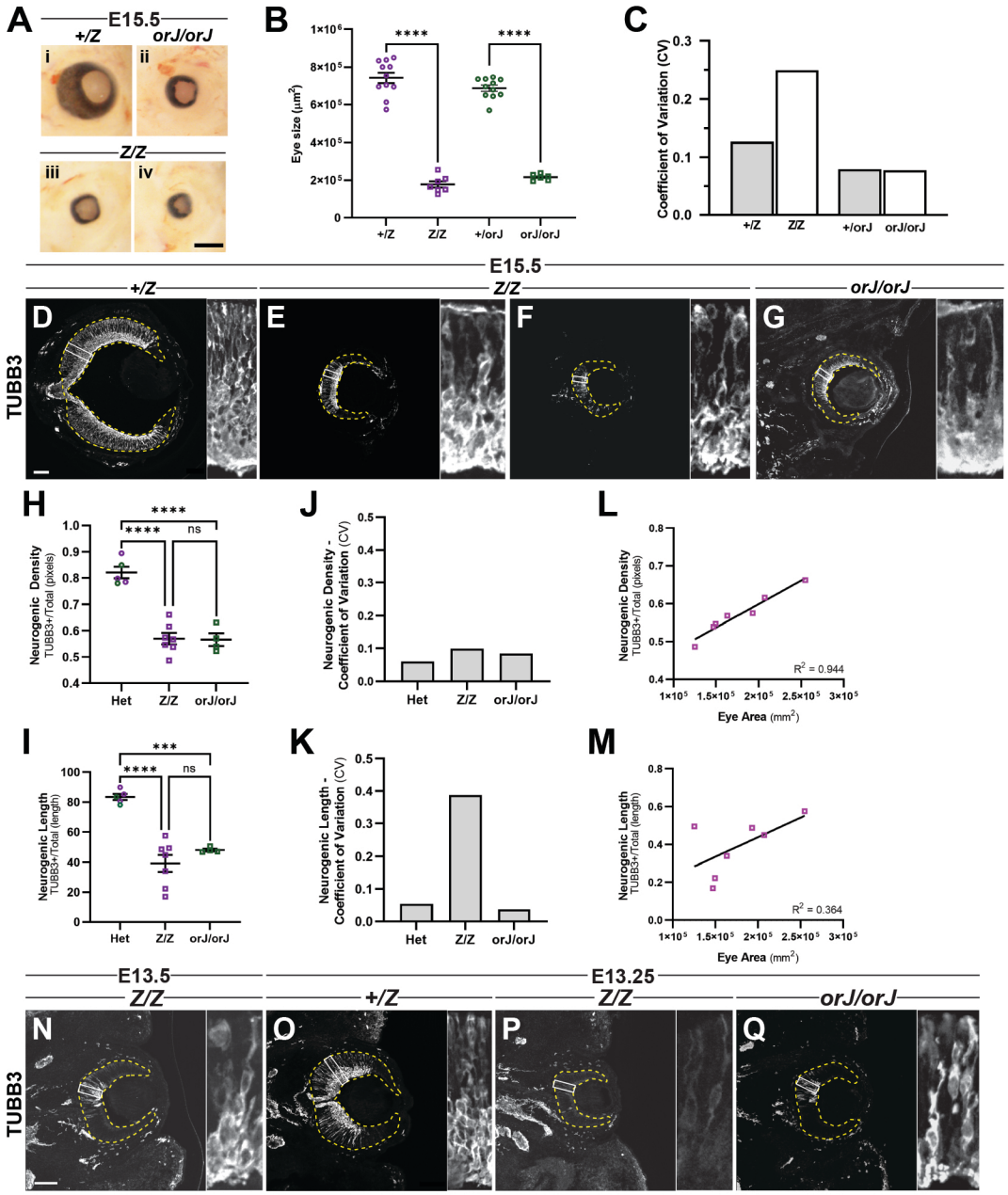
A
E15.5
+/Z
orJ/orJ
i
ii
Z/Z
iii
iv
B
Eye size (μm²)
****
****
+/Z
Z/Z
+/orJ
orJ/orJ
C
Coefficient of Variation (CV)
+/Z
Z/Z
+/orJ
orJ/orJ
E15.5
+/Z
Z/Z
orJ/orJ
TUBB3
D
E
F
G
H
Neurogenic Density
TUBB3+/Total (pixels)
****
****
ns
Het
Z/Z
orJ/orJ
J
Neurogenic Density - Coefficient of Variation (CV)
Het
Z/Z
orJ/orJ
L
Neurogenic Density
TUBB3+/Total (pixels)
R² = 0.944
Eye Area (mm²)
I
Neurogenic Length
TUBB3+/Total (length)
***
****
ns
Het
Z/Z
orJ/orJ
K
Neurogenic Length - Coefficient of Variation (CV)
Het
Z/Z
orJ/orJ
M
Neurogenic Length
TUBB3+/Total (length)
R² = 0.364
Eye Area (mm²)
E13.5
Z/Z
E13.25
+/Z
Z/Z
orJ/orJ
TUBB3
N
O
P
Q

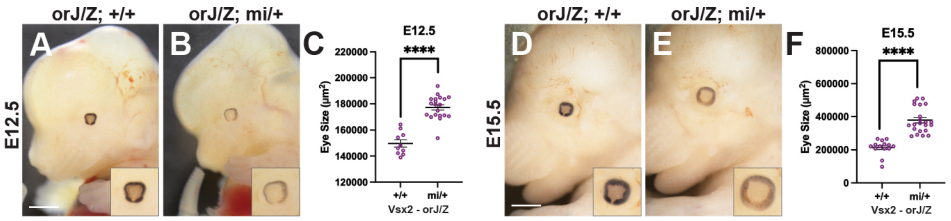
orJ/Z; +/+
orJ/Z; mi/+
A
B
C
E12.5
E12.5
****
Eye Size (µm²)
220000
200000
180000
160000
140000
120000
+/+
mi/+
Vsx2 - orJ/Z
orJ/Z; +/+
orJ/Z; mi/+
D
E
F
E15.5
E15.5
****
Eye Size (µm²)
800000
600000
400000
200000
0
+/+
mi/+
Vsx2 - orJ/Z

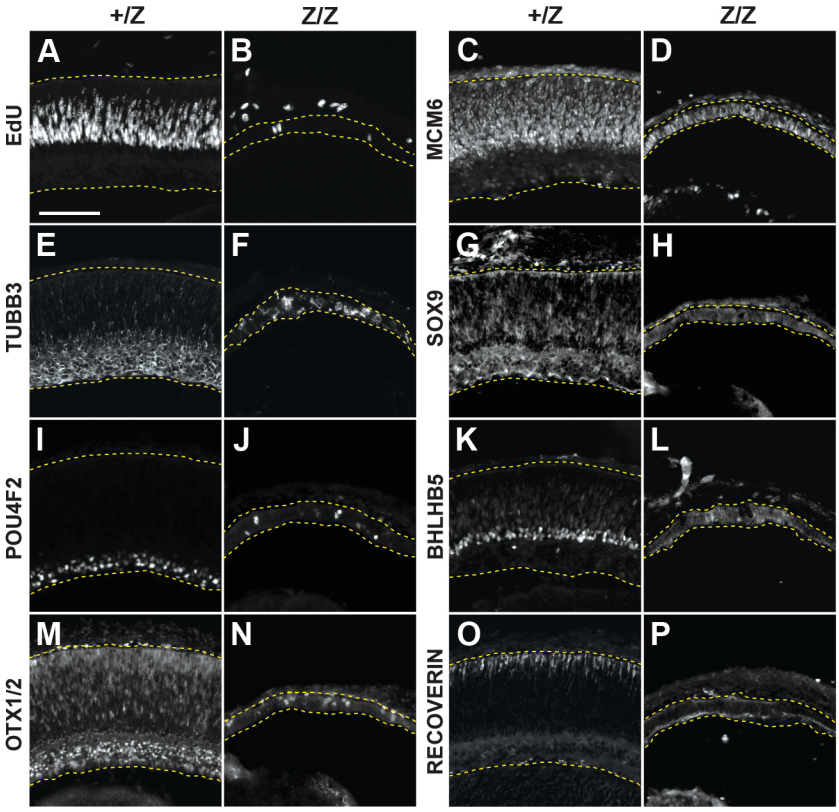
+/Z
Z/Z
+/Z
Z/Z
A
B
C
D
EdU
MCM6
E
F
G
H
TUBB3
SOX9
I
J
K
L
POU4F2
BHLHB5
M
N
O
P
OTX1/2
RECOVERIN

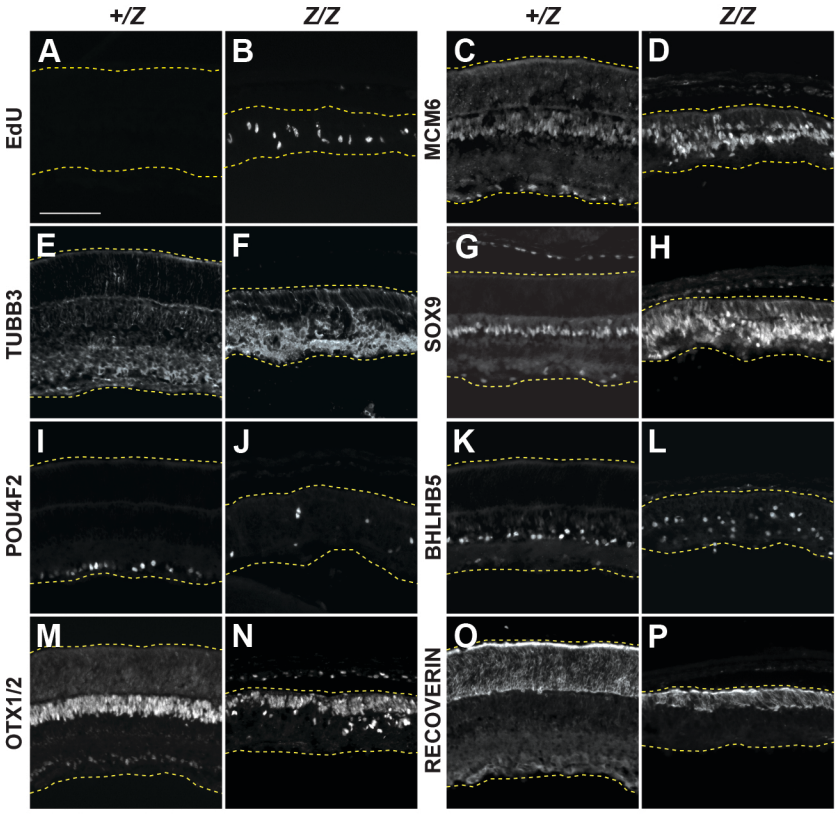
+/Z
Z/Z
+/Z
Z/Z
A
B
C
D
EdU
MCM6
E
F
G
H
TUBB3
SOX9
I
J
K
L
POU4F2
BHLHB5
M
N
O
P
OTX1/2
RECOVERIN

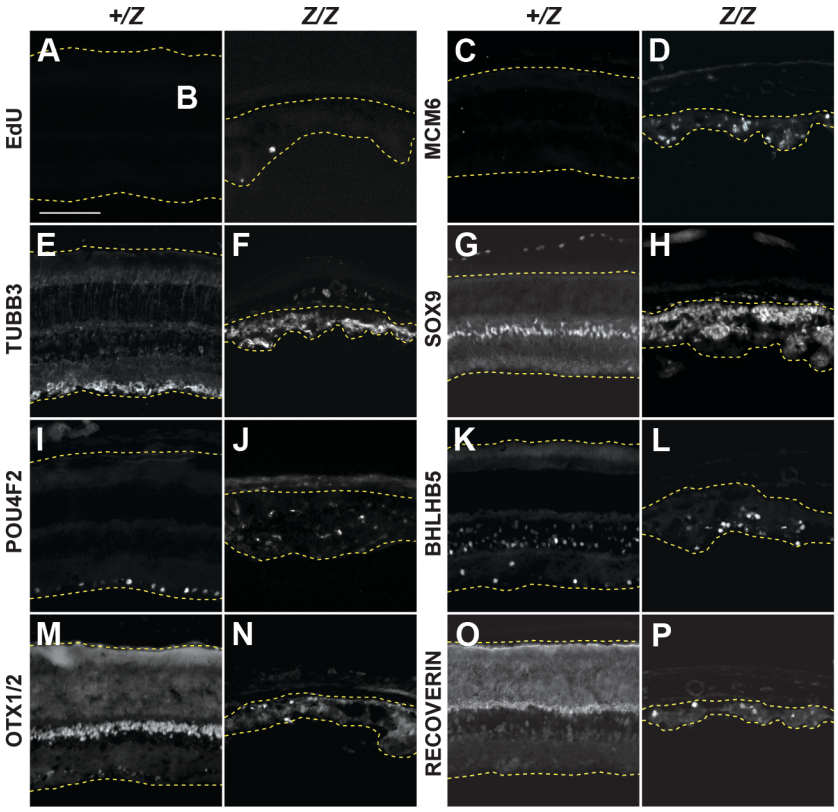
+/Z
Z/Z
+/Z
Z/Z
EdU
MCM6
TUBB3
SOX9
POU4F2
BHLHB5
OTX1/2
RECOVERIN
A
B
C
D
E
F
G
H
I
J
K
L
M
N
O
P

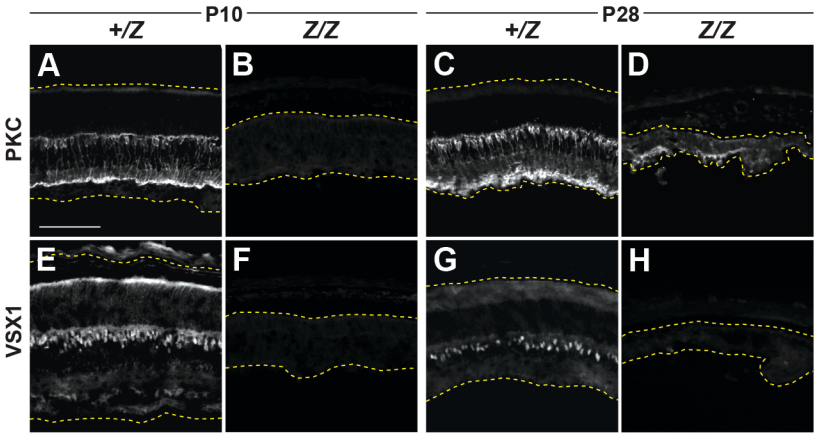
P10
P28
+/Z
Z/Z
+/Z
Z/Z
PKC
VSX1
A
B
C
D
E
F
G
H